

Symbol Detection for Massive MIMO AF Relays Using Approximate Bayesian Inference

Haochuan zhang and Qiuyun Zou

Abstract—For massive MIMO AF relays, symbol detection becomes a practical issue when the number of antennas is not large enough, since linear methods are non-optimal and optimal methods are exponentially complex. This paper proposes a new detection algorithm that offers Bayesian-optimal MSE at the cost of $O(n^3)$ complexity per iteration. The algorithm is in essence a hybrid of two methods recently developed for deep learning, with particular optimization for relay. As a hybrid, it inherits from the two a state evolution formalism, where the asymptotic MSE can be precisely predicted through a scalar equivalent model. The algorithm also degenerates easily to many results well-known when single-hop considered.

Index Terms—Massive MIMO, AF Relay, approximate Bayesian inference, state evolution, deep learning

I. INTRODUCTION

Massive multiple-input multiple-output (MIMO) [1] is currently a compelling sub-6 GHz physical-layer technology for future wireless access, including 5G [2]. It offers many desirable benefits, among which are low complexity processing, excellent spectral efficiency, and superior energy efficiency, by using an unlimited number of antennas [1]. In the technology's practical rolling out, however, only a limited number of antennas (tens to hundreds) was adopted, considering software and hardware limitations. Such an inadequacy in the antenna number poses a critical challenge to symbol detection, a component key to modern digital architecture that recovers/estimates transmitted data from observations corrupted by noise and channel fading. With only a limited number of antennas, simple linear detectors (as advocated by [1]) are far away from optimal since the channel matrix is hardly orthogonal [3]. Theoretically optimal or sub-optimal (nonlinear) detectors, such as the maximum likelihood (ML) and sphere decoding, however, require a computational complexity that grows exponentially with the number of antennas. Considering the case of high-order modulation with several hundreds antennas, this complexity quickly soars up to an unacceptably high level.

One possible way out of the dilemma could be using state-of-the-art algorithms from compressed sensing and artificial intelligence to attain a good approximate Bayesian inference. Among these algorithms are approximate message passing (AMP) [4], expectation propagation (EP) [5] (a.k.a. expectation consistent, EC [6]), and their variants [7], [8], [9], [10], [11], [12]. The AMP class uses a quadratic approximation of the loopy belief propagation to derive an efficient

implementation of the Bayesian estimation, requiring only linear complexity per iteration. Another striking aspect of the AMP class is that their asymptotic mean squared error (MSE) can be accurately tracked by a simple one-dimensional iteration termed state evolution (SE) [13]. EP, on the other hand, originating from variational inference, can be applied to a class of weighting matrices broader than AMP. It also enjoys a MSE performance better than the AMP class, but at a price of increasing complexity that is roughly on the order of $O(n^3)$, with n being the dimension of matrix inversion. Both classes can offer a decent tradeoff between efficiency and effectiveness. For this reason, they were soon introduced to the communications community and had gained their popularity ever since. To name a few of the examples, the AMP class has been successfully applied to symbol detection of massive MIMO in [14], to channel estimation in [15], and to joint channel-and-data detection in [16]. For the EP class, successful applications can be found in [17], [18], [12] and so on. These works, however, all relied on the assumption of a single-hop communication. The methods used cannot be extended to cover the more general framework of multi-hop communications.

Multi-hop communications, a.k.a. relaying, is a key enabler for throughput improvement, as well as coverage enhancement [19]. There are actually two types of relays: one is the amplify-and-forward (AF) (a.k.a. non-regenerative) relay, which simply repeats the physical signal received, and the other is the decode-and-forward (DF) (a.k.a. regenerative) relay that decodes the message before sending it out again. Here we consider AF relay exclusively and assume the use of massive MIMO. Although our method can be easily extended to cover three hops and more, we provide details only for a dual-hop case to ease statements. In the multi-hop massive MIMO setting, we found that previous work were mostly focusing on theoretical analysis [20], [21], with very few on the practical issue of symbol detection. A reason for this would lie in the fundamental limitation that conventional factor graph of the AMP and EP classes involves only two blocks, representing a transmitter and a receiver. No relay is involved or allowed. Given the practical importance of symbol detection in modern digital systems, finding an algorithm that is both effective and efficient, has thus become a issue of urgent need, not only to the industry but also to the academia.

Fortunately, an algorithm termed multi-layer vector AMP (ML-VAMP) [22] may offer a solution, which was recently proposed for deep learning. Belonging to the family of approximate Bayesian inference, the algorithm is capable of handling the concatenation of multiple standard linear models

H. Zhang is with Guangdong University of Technology, Guangzhou 510006, China (email: haochuan.zhang@qq.com).

Q. Zou is with Beijing University of Posts and Telecommunications, Beijing 100876, China (email: qiuyun.zou@bupt.edu.cn).

(i.e., linear mixing plus Gaussian noise) and multiple non-linear activation functions. We find that such a concatenation resembles the multi-hop relay in certain aspects, and also that another algorithm, termed multi-layer generalized expectation consistent (ML-GEC) [23] developed by the authors of this paper, further provides a framework that is more convenient to analyze. The ML-GEC extends the ML-VAMP to cover an even broader scope of system models, by introducing some new entities to the message updating process. Inspired by these two works, this paper proposes a new algorithm that can efficiently detect the modulated symbols of massive MIMO relays when the number of antennas is median. The algorithm proposed is in essence a hybrid of the ML-VAMP and the ML-GEC, with certain particular optimization for the relay massive case. In an iterative manner it deliver message from each hop to the entire network and fulfil in effect a joint detection of all hops. As a hybrid, the algorithm enjoys many common superiorities from the previous two. One remarkable superiority is a good efficient-effective tradeoff. The mean squared error (MSE) of the algorithm's output is Bayesian optimal while the computational complexity is under $O(n^3)$ per iteration, with n denoting the antenna numbers. Another superiority is the theoretical predictability of the algorithm's asymptotic behavior. In large dimension, its MSE can be exactly predicted through the recursion of certain one-dimension equations, termed state evolution. It is also worthy of noting that, the algorithm, taking dual-hop for illustration, is readily extendable to the general case of multi-hop. Furthermore, when considering single-hop, it degenerates smoothly to the well-known results of EP [18] and VAMP [24].

Notations: $(\cdot)^H$ refers to conjugate transpose. \propto means proportional to. $\text{Diag}(\mathbf{v})$ refers to the diagonal matrix with \mathbf{v} on its diagonal positions, while $\text{diag}(\mathbf{A})$ is a vector of the diagonal elements of \mathbf{A} . \odot denotes componentwise multiplication, while \oslash for division. $\mathcal{N}_c(\mathbf{x}|\boldsymbol{\mu}, \boldsymbol{\Sigma})$ denotes the complex Gaussian density with argument \mathbf{x} , mean $\boldsymbol{\mu}$, and covariance $\boldsymbol{\Sigma}$. We also abuse the notation $\mathcal{N}_c(\mathbf{x}|\boldsymbol{\mu}, \boldsymbol{\sigma})$ to a Gaussian density whose covariance is a diagonal matrix with $\boldsymbol{\sigma}$ on the diagonal.

$$\mathbb{E}[\mathbf{x} | \mathbf{m}, \mathbf{v}, \mathcal{F}(\cdot)] = \frac{\int \mathbf{x} \mathcal{N}(\mathbf{x}|\mathbf{m}, \mathbf{v}) \mathcal{F}(\mathbf{x}) d\mathbf{x}}{\int \mathcal{N}(\mathbf{x}|\mathbf{m}, \mathbf{v}) \mathcal{F}(\mathbf{x}) d\mathbf{x}} \quad (1a)$$

$$\text{Var}[\mathbf{x} | \mathbf{m}, \mathbf{v}, \mathcal{F}(\cdot)] = \frac{\int \mathbf{x} \mathbf{x}^H \mathcal{N}(\mathbf{x}|\mathbf{m}, \mathbf{v}) \mathcal{F}(\mathbf{x}) d\mathbf{x}}{\int \mathcal{N}(\mathbf{x}|\mathbf{m}, \mathbf{v}) \mathcal{F}(\mathbf{x}) d\mathbf{x}} - \mathbb{E}[\mathbf{x} | \mathbf{m}, \mathbf{v}, \mathcal{F}(\cdot)] \cdot \mathbb{E}^H[\mathbf{x} | \mathbf{m}, \mathbf{v}, \mathcal{F}(\cdot)] \quad (1b)$$

II. SYSTEM MODEL

In this paper, we consider massive MIMO AF relays using a median number of antennas. We take dual-hop as an illustrating example and the system model is

$$\text{First hop : } \mathbf{y} = \mathbf{Q}(\mathbf{H}\mathbf{x} + \mathbf{w}??) \quad (2)$$

$$\text{Second hop : } \mathbf{z} = \mathbf{C}\mathbf{y} + \mathbf{n} \quad (3)$$

where $\mathbf{x} \in \mathbb{C}^L$, $\mathbf{y} \in \mathbb{C}^M$, and $\mathbf{z} \in \mathbb{C}^N$ are the symbol vectors sent from the source node, repeated by the relay node, and received at the destination node, respectively. $\mathbf{H} \in \mathbb{C}^{M \times L}$

and $\mathbf{C} \in \mathbb{C}^{N \times M}$ are the channel matrices of the 1st and the 2nd hops respectively. $\mathbf{w} \in \mathbb{C}^M$ and $\mathbf{n} \in \mathbb{C}^N$ are the additive white Gaussian noise (AWGN), with $\mathbf{w} \sim \mathcal{N}_c(\mathbf{0}, \sigma_1^2 \mathbf{I})$ and $\mathbf{n} \sim \mathcal{N}_c(\mathbf{0}, \sigma_2^2 \mathbf{I})$ being known to the destination node. The elements of the random vector \mathbf{x} are independent and non-sparse (as opposed to compressed sensing), where $p(\mathbf{x}) = \prod_{i=1}^M p_i(x_i)$. Given this non-sparsity, an additional condition is imposed on the dimensions, $L \leq M \leq N$, to make the detection non-trivial. In AF relays, the vector \mathbf{z} is observed (known), while the interim result \mathbf{y} is hidden (unknown) from the destination node. We also assume the destination node to have perfect channel state information (CSI) about both hops. In practice, this CSI can be obtained by using channel estimators particularly designed for MIMO AF relays [25].

In this paper, we aim at getting a Bayesian-optimal posterior mean estimate (PME) (optimal in the Bayesian sense) for each element x_i of \mathbf{x} , given the observation \mathbf{z} , the channels, and the noise variances:

$$\hat{x}_i = \mathbb{E}_{x_i|\mathbf{z}}[x_i] \quad (4)$$

where the expectation is taken w.r.t. a marginal posterior density, $p(x_i|\mathbf{z})$, defined as

$$p(x_i|\mathbf{z}) \propto \int_{\mathbf{x}_{\sim i}} d\mathbf{x}_{\sim i} \int_{\mathbf{t}} d\mathbf{t} \int_{\mathbf{y}} p(\mathbf{x}) p(\mathbf{t}|\mathbf{x}) p(\mathbf{y}|\mathbf{t}) p(\mathbf{z}|\mathbf{y}) d\mathbf{y} \quad (5)$$

with $p(\mathbf{t}|\mathbf{x}) = \delta(\mathbf{t} - \mathbf{H}\mathbf{x})$, $p(\mathbf{y}|\mathbf{t}) = \mathcal{N}_c(\mathbf{y}; \mathbf{t}, \sigma_1^2 \mathbf{I})$, and $p(\mathbf{z}|\mathbf{y}) = \mathcal{N}_c(\mathbf{z}; \mathbf{C}\mathbf{y}, \sigma_2^2 \mathbf{I})$. The main difficulty in evaluating the multi-fold integral comes from two facts, first the high dimension of the vectors (i.e., antenna numbers), and second the large cardinality of the integral domain (i.e., the modulation order). The overall complexity is on the order of cardinality to dimension, which grows exponentially fast and makes the direct computation almost impossible. An alternative solution to this problem is to use factor graph and message passing.

III. THE PROPOSED ALGORITHM

A. Algorithm

A factor graph associated with the density (5) is given in Fig. 1. There are two kinds of nodes in the figure, the variable nodes, and the factor nodes. Both nodes are in vector form, with a detailed description for the message updating also in Fig. 1. Here, we note that the variable nodes are transparent to the message passing. By contrast, a factor node will "combine" all messages received (from both directions) with its own (inherited from the factor function), get a joint "information," subtract from it the incoming message in each direction by turns, and finally feeds back the "extrinsic" information to each direction. We call the delivery of a message from the left to the right in the factor graph a "forward passing," and its opposite the "back passing." Connecting a forward and a back passing, ones gets an iteration of the algorithm. It is also worthy of noting that the messages delivered are indeed Gaussian densities, which means only the mean and the variance are needed. To approximate a general function $q(\cdot)$ by a Gaussian density, we adopt the same projection technique as [26], where

$$\text{Proj}_{\mathbf{x}}[q(\mathbf{x})] = \arg \min_{p(\mathbf{x}) \in \Phi} \mathcal{D}_{\text{KL}}(q(\mathbf{x})||p(\mathbf{x})) \quad (6)$$

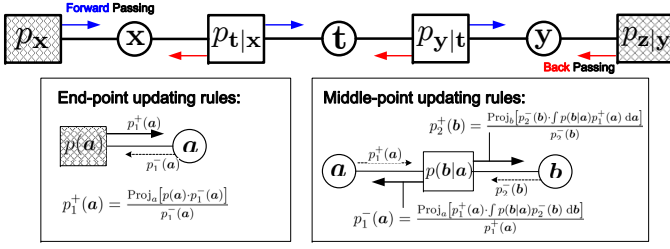


Fig. 1. Factor graph in vector form and message updating rules

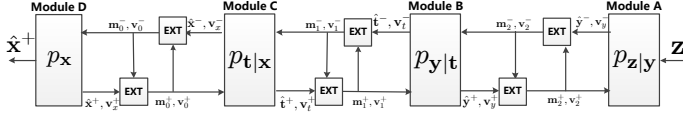


Fig. 2. Block diagram of the proposed algorithm

with Φ being the set of Gaussian densities in \mathbf{x} , and $\mathcal{D}_{\text{KL}}(q||p)$ being the Kullback-Leibler divergence, a measure of how one probability distribution $q(\mathbf{x})$, diverges from a second, expected probability distribution $p(\mathbf{x})$. Based on this factor graph and its message passing rules, we proposed a new method, Algorithm 1, to solve the PME problem in (4). Some key steps of the derivations are given in Appendix A. Here we note that the expectation in (21) is taken w.r.t. a density proportional to $p(\mathbf{x})\mathcal{N}_c(\mathbf{x}|\mathbf{m}_0^-, \mathbf{v}_0^-)$, and so is the variance in (22).

B. Block Diagram

To better illustrate the working mechanism of our algorithm, also to shed light on the software and hardware implementation, we provide in Fig. 2 a block diagram of the algorithm. In the diagram, Module A corresponds to (8)-(9) of Algorithm 1, with Module B to (12)-(13) and (31)-(32), Module C to (17)-(18) and (27)-(28), and Module D to (21)-(22). Some discussions on the diagram are also given below.

- The algorithm proposed, indeed, provides an iterative manner of jointly estimating the 1st and the 2nd hops, with $\hat{\mathbf{x}}$ and $\hat{\mathbf{y}}$ as the estimated results. The rationale behind a joint estimation to outperform algorithms which handle each hop separately is that more information can be utilized by each part of the network, and a global optima is more likely to be attained. The superiority of our joint processing will be discussed with more details in Section IV.
- A key step in our iterative algorithm is to compute the *extrinsic* message, represented by $\boxed{\text{EXT}}$. This operation bears a similarity to the turbo-like processing, which allows only the extrinsic information to traverse the network, suppressing error propagation to the minimum. The computation is formally defined as $(\mathbf{m}_1, \mathbf{v}_1) \boxed{\text{EXT}} (\mathbf{m}_2, \mathbf{v}_2) = [\mathbf{v}_3 \odot (\mathbf{m}_1 \otimes \mathbf{v}_1 - \mathbf{m}_2 \otimes \mathbf{v}_2), \mathbf{v}_3]$, with $\mathbf{v}_3 = \mathbf{1} \otimes (\mathbf{1} \otimes \mathbf{v}_1 - \mathbf{1} \otimes \mathbf{v}_2)$.
- Most computational burden of the proposed algorithm comes from Module C in the diagram. To be specific, the matrix inversions in (7), (16), and (25) of Algorithm

Algorithm 1 The proposed algorithm

1. Initialization: $\mathbf{v}_2^+ = \mathbf{1}$, $\mathbf{v}_1^+ = \mathbf{1}$, $\mathbf{v}_0^+ = \mathbf{1}$, $\mathbf{m}_2^+ = \mathbf{0}$, $\mathbf{m}_1^+ = \mathbf{0}$, and $\mathbf{m}_0^+ = \mathbf{0}$.
2. Iteration (for $k = 1 \dots, K$)

(1) Back passing

$$\mathbf{Q}_y^- = (\sigma_2^{-2} \mathbf{C}^H \mathbf{C} + \text{Diag}(\mathbf{1} \otimes \mathbf{v}_2^+))^{-1} \quad (7)$$

$$\hat{\mathbf{y}}^- = \mathbf{Q}_y^- (\sigma_2^{-2} \mathbf{C}^H \mathbf{z} + \mathbf{m}_2^+ \otimes \mathbf{v}_2^+) \quad (8)$$

$$\mathbf{v}_y^- = \text{diag}(\mathbf{Q}_y^-). \quad (9)$$

$$\mathbf{v}_2^- = \mathbf{1} \otimes (\mathbf{1} \otimes \mathbf{v}_y^- - \mathbf{1} \otimes \mathbf{v}_2^+) \quad (10)$$

$$\mathbf{m}_2^- = \mathbf{v}_2^- \odot (\hat{\mathbf{y}}^- \otimes \mathbf{v}_y^- - \mathbf{m}_2^+ \otimes \mathbf{v}_2^+) \quad (11)$$

$$\mathbf{v}_t^- = \mathbf{1} \otimes (\mathbf{1} \otimes \mathbf{v}_1^+ + \mathbf{1} \otimes (\sigma_1^2 \mathbf{1} + \mathbf{v}_2^-)) \quad (12)$$

$$\hat{\mathbf{t}}^- = \mathbf{v}_t^- \odot (\mathbf{m}_1^+ \otimes \mathbf{v}_1^+ + \mathbf{m}_2^- \otimes (\sigma_1^2 \mathbf{1} + \mathbf{v}_2^-)) \quad (13)$$

$$\mathbf{v}_1^- = \mathbf{1} \otimes (\mathbf{1} \otimes \mathbf{v}_t^- - \mathbf{1} \otimes \mathbf{v}_1^+) \quad (14)$$

$$\mathbf{m}_1^- = \mathbf{v}_1^- \odot (\hat{\mathbf{t}}^- \otimes \mathbf{v}_t^- - \mathbf{m}_1^+ \otimes \mathbf{v}_1^+) \quad (15)$$

$$\mathbf{Q}_x^- = (\mathbf{H}^H \text{Diag}(\mathbf{1} \otimes \mathbf{v}_1^-) \mathbf{H} + \text{Diag}(\mathbf{1} \otimes \mathbf{v}_0^+))^{-1} \quad (16)$$

$$\hat{\mathbf{x}}^- = \mathbf{Q}_x^- (\mathbf{H}^H \text{Diag}(\mathbf{1} \otimes \mathbf{v}_1^-) \mathbf{m}_1^- + \mathbf{m}_0^+ \otimes \mathbf{v}_0^+) \quad (17)$$

$$\mathbf{v}_x^- = \text{diag}(\mathbf{Q}_x^-) \quad (18)$$

$$\mathbf{v}_0^- = \mathbf{1} \otimes (\mathbf{1} \otimes \mathbf{v}_x^- - \mathbf{1} \otimes \mathbf{v}_0^+) \quad (19)$$

$$\mathbf{m}_0^- = \mathbf{v}_0^- \odot (\hat{\mathbf{x}}^- \otimes \mathbf{v}_x^- - \mathbf{m}_0^+ \otimes \mathbf{v}_0^+) \quad (20)$$

(2) Forward Passing

$$\hat{\mathbf{x}}^+ = \mathbb{E}[\mathbf{x}|\mathbf{m}_0^-, \mathbf{v}_0^-] \quad (21)$$

$$\mathbf{v}_x^+ = \text{Var}[\mathbf{x}|\mathbf{m}_0^-, \mathbf{v}_0^-] \quad (22)$$

$$\mathbf{v}_0^+ = \mathbf{1} \otimes (\mathbf{1} \otimes \mathbf{v}_x^+ - \mathbf{1} \otimes \mathbf{v}_0^-) \quad (23)$$

$$\mathbf{m}_0^+ = \mathbf{v}_0^+ \odot (\hat{\mathbf{x}}^+ \otimes \mathbf{v}_x^+ - \mathbf{m}_0^- \otimes \mathbf{v}_0^-) \quad (24)$$

$$\mathbf{Q}_x^+ = (\mathbf{H}^H \text{Diag}(\mathbf{1} \otimes \mathbf{v}_1^-) \mathbf{H} + \text{Diag}(\mathbf{1} \otimes \mathbf{v}_0^+))^{-1} \quad (25)$$

$$\mathbf{x}^+ = \mathbf{Q}_x^+ (\mathbf{H}^H \text{Diag}(\mathbf{1} \otimes \mathbf{v}_1^-) \mathbf{m}_1^- + \mathbf{m}_0^+ \otimes \mathbf{v}_0^+) \quad (26)$$

$$\hat{\mathbf{t}}^+ = \mathbf{H} \mathbf{x}^+ \quad (27)$$

$$\mathbf{v}_t^+ = \text{diag}(\mathbf{H} \mathbf{Q}_x^+ \mathbf{H}^H) \quad (28)$$

$$\mathbf{v}_1^+ = \mathbf{1} \otimes (\mathbf{1} \otimes \mathbf{v}_t^+ - \mathbf{1} \otimes \mathbf{v}_1^-) \quad (29)$$

$$\mathbf{m}_1^+ = \mathbf{v}_1^+ \odot (\hat{\mathbf{t}}^+ \otimes \mathbf{v}_t^+ - \mathbf{m}_1^- \otimes \mathbf{v}_1^-) \quad (30)$$

$$\mathbf{v}_y^+ = \mathbf{1} \otimes ((\mathbf{1} \otimes \mathbf{v}_2^-) + \mathbf{1} \otimes (\mathbf{v}_1^+ + \sigma_1^2 \mathbf{1})) \quad (31)$$

$$\hat{\mathbf{y}}^+ = \mathbf{v}_y^+ \odot (\mathbf{m}_1^+ \otimes (\mathbf{v}_1^+ + \sigma_1^2 \mathbf{1}) + \mathbf{m}_2^- \otimes \mathbf{v}_2^-) \quad (32)$$

$$\mathbf{v}_2^+ = \mathbf{1} \otimes (\mathbf{1} \otimes \mathbf{v}_y^+ - \mathbf{1} \otimes \mathbf{v}_2^-) \quad (33)$$

$$\mathbf{m}_2^+ = \mathbf{v}_2^+ \odot (\hat{\mathbf{y}}^+ \otimes \mathbf{v}_y^+ - \mathbf{m}_2^- \otimes \mathbf{v}_2^-) \quad (34)$$

3. Output: $\hat{\mathbf{x}}^+$.

1 all have a complexity on the order of $O(n^3)$, with n denoting the dimension of the matrix involved. This complexity, originating from EP [5], seems to be inherited by ML-VAMP [22] and ML-GEC [23]. Fortunately, a new approach to avoid the matrix inversion has been developed in [27] very recently. That approach is also applicable to the algorithm here, but we save it for further studies.

- Given the block diagram, we now explain why the proposed algorithm is a hybrid of the ML-VAMP [22]

and the ML-GEC [23] with particular optimization for relay massive. There are at least three facets. First, the proposed algorithm removes the (deep learning) activation functions from the ML-VAMP since it is not needed here. Second, after the removal above, it follows the same procedure as the ML-GEC to update the message of most factor nodes except the last two. Third, it merges the ML-GEC's last two factors nodes to be a single one, i.e., Module A in Fig. 2, shortening the entire message passing route.

- Relay or multi-hop communication is a general framework that embraces the single-hop. It is worthy of noting our algorithm can be generalized directly to cover multi-hop, although Fig. 2 only gives a dual-hop example. The generation to m -hop is done by first creating $m-1$ copies of the Module B and C pair, then changing the channel matrix and noise variance for each pair accordingly, and finally concatenating them in ascending order of the hop indices. We also note that our algorithm degenerates easily to the well-known results for single-hop. To see this, one only needs to take out Module B and C. After that, another algorithm (block diagram also) is immediately seen, which is exactly the same as EP [18] and VAMP [24].

C. State Evolution

Inheriting from the AMP and the EP classes, the proposed algorithm admits an exact description of the high-dimensional behavior. Specifically, the variance of the output can be computed through a one-dimensional recursion, i.e., the SE.

To this end, a scalar system model and some new parameters are introduced. The scalar model is: $r = x + w$, with $w \sim \mathcal{N}_c(0, v_0^-)$. The PME output then becomes $\mathbb{E}[x|r] = \int x p(x)p(r|x) dx$, with the MSE given by $\text{MSE}(v_0^-) = \mathbb{E}[|x - \mathbb{E}[x|r]|^2]$, where the expectation is taken w.r.t. $p(r, x) = p(x)p(r|x)$. We denote λ_i as the i -th eigenvalue of $\mathbf{H}^H \mathbf{H}$, and η_i as that of $\mathbf{C}^H \mathbf{C}$. We also define $\langle f(\lambda_i) \rangle_N \triangleq \frac{1}{N} \sum_{i=1}^N f(\lambda_i)$. Then, we derive the SE for the proposed algorithm. The results are given in Algorithm 2. Details of the derivation are omitted here. Similar techniques as in [11] can be applied to the current case, while one has to go through the derivations from the beginning.

IV. NUMERICAL RESULTS

In this section, we carry out numerical simulations and compare the results with other competing methods to verify the effectiveness of Algorithm 1. Three algorithms, upon which linear/nonlinear and separate-/joint-processing are applied, are chosen to differentiate from our iterative (nonlinear) joint estimation¹. These three are:

¹ As mentioned earlier, our algorithm is a hybrid of the ML-VAMP and the ML-GEC, with particular optimization to a shorten the message passing route. The computational complexity is reduced after the removal and mergence of factor nodes; however, it remains on the same same order (due to the same bottleneck of matrix inversion). The BER/MSE performance of the three is also similar. For this reason, we omit the comparison among the three, but focusing more on their difference to techniques in other class.

Algorithm 2 State Evolution

1. Initial: $k=0$, $\gamma_2^+ = 1$, $\gamma_1^+ = 1$, $\gamma_0^+ = 1$
2. Iteration (for $k = 1 : K$)

Back Passing

$$q_y^- = \langle 1/(\sigma_2^{-2} \eta_i + \gamma_2^+) \rangle_M \quad (35)$$

$$\gamma_2^- = 1/q_y^- - \gamma_2^+ \quad (36)$$

$$\gamma_t^- = \gamma_1^+ + \gamma_2^- / (1 + \gamma_2^- \sigma_1^2) \quad (37)$$

$$\gamma_1^- = \gamma_t^- - \gamma_1^+ \quad (38)$$

$$q_x^- = \langle 1/(\lambda_i \gamma_1^- + \gamma_0^+) \rangle_M \quad (39)$$

$$\gamma_0^- = \frac{1}{q_x^-} - \gamma_0^+ \quad (40)$$

Forward Passing

$$\gamma_0^+ = 1/\text{MSE}(\gamma_0^-) - \gamma_0^- \quad (41)$$

$$q_t^+ = \langle \lambda_i / (\lambda_i \gamma_1^- + \gamma_0^+) \rangle_L \quad (42)$$

$$\gamma_1^+ = 1/q_t^+ - \gamma_1^- \quad (43)$$

$$\gamma_y^+ = \gamma_2^- + \gamma_1^+ / (1 + \gamma_1^+ \sigma_1^2) \quad (44)$$

$$\gamma_2^+ = \gamma_y^+ - \gamma_2^- \quad (45)$$

3. Output: $\text{MSE}(\gamma_0^-)$
-

- **LMMSE+LS** (linear, separate): Perform LS estimation on the 2nd hop, and use the result as the 1st hop's observation, to later perform an LMMSE estimation on the 1st hop (Performing LMMSE also on the 2nd hop is difficult due to the lack of \mathbf{y} 's prior information).
- **Single-LMMSE** (linear, joint): Instead of separating the two hops, use a compound model of $\mathbf{z} = \mathbf{C}^H \mathbf{H} \mathbf{x} + \mathbf{C}^H \mathbf{w} + \mathbf{n}$, and simply treat the colored noise $\mathbf{C}^H \mathbf{w} + \mathbf{n}$ as a white one with equivalent variance, then perform a single LMMSE estimation over the entire link.
- **EP+LS** (nonlinear, separate): Similar to the LMMSE+LS above, with LS replaced with EP [18], which is nonlinear.

In the numerical simulations, we fix the antenna numbers of the source, relay, and destination at $L = 128$, $M = 256$, and $N = 512$, respectively. Uncorrelated flat Rayleigh fading channels and QPSK without channel coding are assumed. The SNR of the 1st and 2nd hops are denoted as SNR_1 and SNR_2 , respectively.

Fig. 3 compares the bit error rate (BER) of all the four algorithms. Clearly, the proposed algorithm outperforms the other three in BER over the entire SNR range. LMMSE+LS is the worst, with Single-LMMSE only slightly better. These two algorithms both suffer from the non-optimality of the LMMSE, and thus, it is not surprising that, replacing LMMSE with EP (proved to be a better technique [18]) yields a much better algorithm. EP+LS, however, is still inferior to the proposed algorithm. This inferiority could be attributed to the noise augmentation of the LS method in the 2nd hop.

To gain more insights into the proposed algorithm's behavior, we fix the SNR_2 at three levels, i.e., 6dB, 9dB, and 12dB, and vary the SNR_1 from 0 to 20 dB. The BER verse SNR_1 results are presented in Fig. 4. We find that, firstly, the proposed algorithm outperforms EP+LS in all cases and over

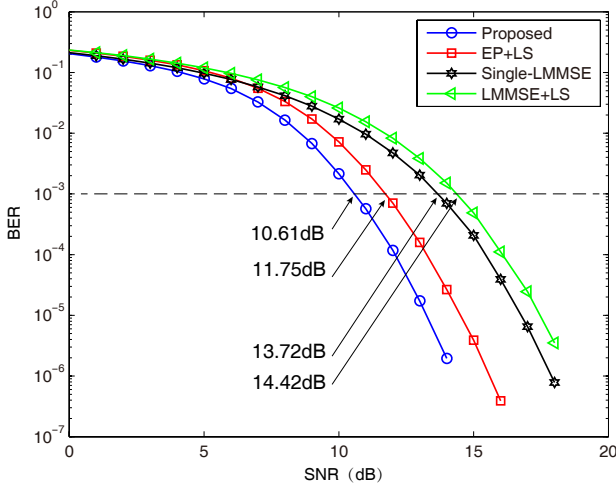


Fig. 3. Comparison of BER performance ($\text{SNR}_2 = \text{SNR}_1 - 3\text{dB}$).

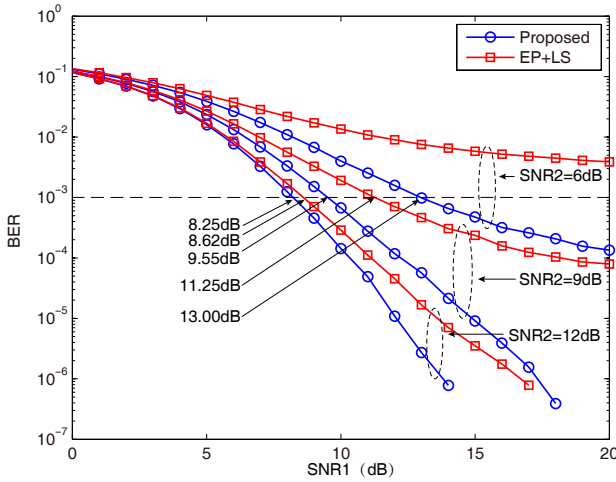


Fig. 4. BER of the EP+LS and the proposed algorithm

the entire SNR range. Secondly, the difference between the two tends to diminish as the SNR_2 soars up. This phenomenon also meets our expectation that as the SNR_2 increases, the LS estimation is becoming more and the more accurate, leaving little room for improvement. In other words, the proposed algorithm differs from the EP+LS in the 2nd hop processing, where the proposed algorithm implicitly utilizes some statistical information about the 2nd hop's input \mathbf{y} in the detection process, while the EP+LS has nothing in prior to depend on (except the channel matrix).

In Fig. 5, we provide a closer look at the proposed algorithm's output MSE per iteration. We find that the algorithm has a quick convergence. Only 5 iterations or less are needed in all cases simulated. Moreover, the algorithm's real MSE per iteration matches perfectly with the one theoretically obtained through state evolution.

V. CONCLUSIONS

This paper considered the problem of symbol detection in the context of massive MIMO AF relays using a median number of antennas. A new algorithm has been proposed to

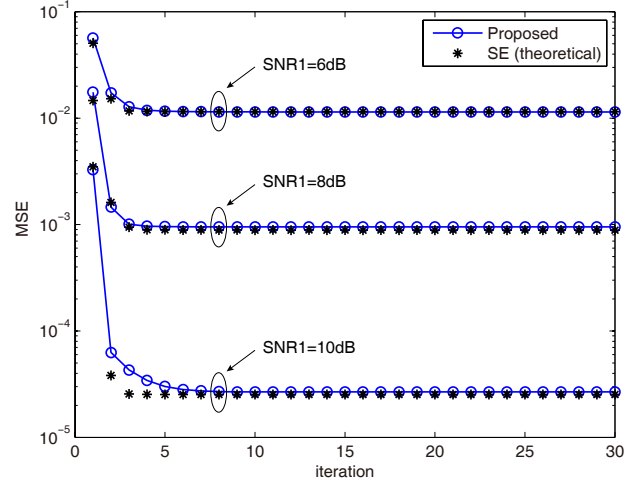


Fig. 5. MSE of the proposed algorithm ($\text{SNR}_2 = 20\text{dB}$)

optimize the tradeoff between effectiveness and efficiency. It can attain Bayesian-optimal MSE at only the cost of $O(n^3)$ complexity. The algorithm is in essence a hybrid of ML-VAMP and ML-GEC, with particular optimization for the massive MIMO relay case. As a hybrid, it inherits from the two the formulism of state evolution, i.e., the asymptotic MSE behavior of the algorithm can be precisely predicted through a scalar equivalent model. Furthermore, it can smoothly degenerate to the well-known result of EP and VAMP when single-hop communication is considered.

APPENDIX A GENERAL DERIVATION

A. Back passing

The belief distribution at the factor node $p(\mathbf{z}|\mathbf{y}) = \mathcal{N}_c(\mathbf{C}\mathbf{y}|\mathbf{z}, \sigma_2^2\mathbf{1})$, i.e., Module A in Fig. 2, is

$$\mathcal{N}_c(\mathbf{y}|\hat{\mathbf{y}}^-, \mathbf{v}_y^-) = \text{Proj}_{\mathbf{y}} [p(\mathbf{z}|\mathbf{y})\mathcal{N}(\mathbf{y}|\mathbf{m}_2^+, \mathbf{v}_2^+)] \quad (46)$$

which can be computed via the use of the Gaussian reproduction property [28]². The result is

$$\hat{\mathbf{y}}^- = \mathbf{Q}_y^- (\sigma_2^{-2}\mathbf{C}^H\mathbf{z} + \mathbf{m}_2^+ \odot \mathbf{v}_2^+) \quad (47)$$

$$\mathbf{v}_y^- = \text{diag}(\mathbf{Q}_y^-). \quad (48)$$

with $\mathbf{Q}_y^- = (\sigma_2^{-2}\mathbf{C}^H\mathbf{C} + \text{Diag}(\mathbf{1} \odot \mathbf{v}_2^+))^{-1}$. After that, the back-passing extrinsic message can be computed as

$$\mathcal{N}_c(\mathbf{y}|\mathbf{m}_2^-, \mathbf{v}_2^-) \propto \frac{\mathcal{N}_c(\mathbf{y}|\hat{\mathbf{y}}^-, \mathbf{v}_y^-)}{\mathcal{N}_c(\mathbf{y}|\mathbf{m}_2^+, \mathbf{v}_2^+)} \quad (49)$$

with the result being

$$\mathbf{v}_2^- = \mathbf{1} \odot (\mathbf{1} \odot \mathbf{v}_y^- - \mathbf{1} \odot \mathbf{v}_2^+) \quad (50)$$

$$\mathbf{m}_2^- = \mathbf{v}_2^- \odot (\hat{\mathbf{y}}^- \odot \mathbf{v}_y^- - \mathbf{m}_2^+ \odot \mathbf{v}_2^+) \quad (51)$$

We move on to the factor node $p(\mathbf{y}|\mathbf{t})$, i.e., Module B,

$$\mathcal{N}_c(\mathbf{t}|\hat{\mathbf{t}}^-, \mathbf{v}_t^-) = \text{Proj}_{\mathbf{t}} [\mathcal{N}_c(\mathbf{t}|\mathbf{m}_1^+, \mathbf{v}_1^+)\mathcal{L}(\mathbf{t})] \quad (52)$$

² Gaussian reproduction property: $\mathcal{N}_c(\mathbf{x}|\mathbf{a}, \mathbf{A})\mathcal{N}_c(\mathbf{x}|\mathbf{b}, \mathbf{B}) = \alpha \cdot \mathcal{N}_c(\mathbf{x}|\mathbf{c}, \mathbf{C})$, where $\alpha = \mathcal{N}_c(\mathbf{0}|\mathbf{a} - \mathbf{b}, \mathbf{A} + \mathbf{B})$, $\mathbf{c} = (\mathbf{A}^{-1} + \mathbf{B}^{-1})^{-1}(\mathbf{A}^{-1}\mathbf{a} + \mathbf{B}^{-1}\mathbf{b})$, and $\mathbf{C} = (\mathbf{A}^{-1} + \mathbf{B}^{-1})^{-1}$.

where $\mathcal{L}(\mathbf{t}) \triangleq \int_{\mathbf{y}} p(\mathbf{y}|\mathbf{t}) \mathcal{N}_c(\mathbf{y}|\mathbf{m}_2^-, \mathbf{v}_2^-) d\mathbf{y}$, and according to our notation systems (1), the mean and variance can be expressed as

$$\hat{\mathbf{t}}^- = \mathbb{E}[\mathbf{t} | \mathbf{m}_1^+, \mathbf{v}_1^+, \mathcal{L}(\cdot)] \quad (53)$$

$$\mathbf{v}_t^- = \text{Var}[\mathbf{t} | \mathbf{m}_1^+, \mathbf{v}_1^+, \mathcal{L}(\cdot)] \quad (54)$$

Then the extrinsic message can be obtained

$$\mathcal{N}_c(\mathbf{t}|\mathbf{m}_1^-, \mathbf{v}_1^-) \propto \frac{\mathcal{N}_c(\mathbf{t}|\hat{\mathbf{t}}^-, \mathbf{v}_t^-)}{\mathcal{N}_c(\mathbf{t}|\mathbf{m}_1^+, \mathbf{v}_1^+)} \quad (55)$$

$$\mathbf{v}_1^- = \mathbf{1} \odot (\mathbf{1} \odot \mathbf{v}_t^- - \mathbf{1} \odot \mathbf{v}_1^+) \quad (56)$$

$$\mathbf{m}_1^- = \mathbf{v}_1^- \odot (\hat{\mathbf{t}}^- \odot \mathbf{v}_t^- - \mathbf{m}_1^+ \odot \mathbf{v}_1^+) \quad (57)$$

We continue with the $p(\mathbf{t}|\mathbf{x}) = \delta(\mathbf{t} - \mathbf{H}\mathbf{x})$ factor node, i.e. Module C,

$$\begin{aligned} & \mathcal{N}_c(\mathbf{x}|\hat{\mathbf{x}}^-, \mathbf{v}_x^-) \\ = & \text{Proj}_{\mathbf{x}} \left[\int_{\mathbf{t}} p(\mathbf{t}|\mathbf{x}) \mathcal{N}_c(\mathbf{x}|\mathbf{m}_0^+, \mathbf{v}_0^+) \mathcal{N}_c(\mathbf{t}|\mathbf{m}_1^-, \mathbf{v}_1^-) d\mathbf{t} \right] \end{aligned} \quad (58)$$

Similarly, we obtain

$$\mathbf{Q}_x^- = (\mathbf{H}^H \text{Diag}(\mathbf{1} \odot \mathbf{v}_1^-) \mathbf{H} + \text{Diag}(\mathbf{1} \odot \mathbf{v}_0^+))^{-1} \quad (59)$$

$$\hat{\mathbf{x}}^- = \mathbf{Q}_x^- (\mathbf{H}^H \text{Diag}(\mathbf{1} \odot \mathbf{v}_1^-) \mathbf{r}_1^- + \mathbf{m}_0^+ \odot \mathbf{v}_0^+) \quad (60)$$

$$\mathbf{v}_x^- = \text{diag}(\mathbf{Q}_x^-) \quad (61)$$

Then, the extrinsic message becomes

$$\mathcal{N}_c(\mathbf{x}|\mathbf{r}_0^-, \mathbf{v}_0^-) \propto \frac{\mathcal{N}_c(\mathbf{x}|\hat{\mathbf{x}}^-, \mathbf{v}_x^-)}{\mathcal{N}_c(\mathbf{x}|\mathbf{m}_0^+, \mathbf{v}_0^+)} \quad (62)$$

$$\mathbf{v}_0^- = \mathbf{1} \odot (\mathbf{1} \odot \mathbf{v}_x^- - \mathbf{1} \odot \mathbf{v}_0^+) \quad (63)$$

$$\mathbf{r}_0^- = \mathbf{v}_0^- \odot (\hat{\mathbf{x}}^- \odot \mathbf{v}_x^- - \mathbf{r}_0^+ \odot \mathbf{v}_0^+) \quad (64)$$

B. Forward passing

We compute the joint message of the factor node $p(\mathbf{x})$, i.e., Module D in Fig. 2,

$$\mathcal{N}_c(\mathbf{x}|\hat{\mathbf{x}}^+, \mathbf{v}_x^+) = \text{Proj}_{\mathbf{x}} [p(\mathbf{x}) \mathcal{N}_c(\mathbf{x}|\mathbf{m}_0^-, \mathbf{v}_0^-)] \quad (65)$$

$$\hat{\mathbf{x}}^+ = \mathbb{E}[\mathbf{x}|\mathbf{m}_0^-, \mathbf{v}_0^-] \quad (66)$$

$$\mathbf{v}_x^+ = \text{diag}(\text{Var}[\mathbf{x}|\mathbf{m}_0^-, \mathbf{v}_0^-]) \quad (67)$$

Then, the extrinsic message can be computed as

$$\mathcal{N}_c(\mathbf{x}|\mathbf{m}_0^+, \mathbf{v}_0^+) \propto \frac{\mathcal{N}_c(\mathbf{x}|\hat{\mathbf{x}}^+, \mathbf{v}_x^+)}{\mathcal{N}_c(\mathbf{x}|\mathbf{m}_0^-, \mathbf{v}_0^-)} \quad (68)$$

$$\mathbf{v}_0^+ = \mathbf{1} \odot (\mathbf{1} \odot \mathbf{v}_x^+ - \mathbf{1} \odot \mathbf{v}_0^-) \quad (69)$$

$$\mathbf{m}_0^+ = \mathbf{v}_0^+ \odot (\hat{\mathbf{x}}^+ \odot \mathbf{v}_x^+ - \mathbf{m}_0^- \odot \mathbf{v}_0^-) \quad (70)$$

We move on to the factor node $p(\mathbf{t}|\mathbf{x}) = \delta(\mathbf{t} - \mathbf{H}\mathbf{x})$, i.e., Module C,

$$\begin{aligned} & \mathcal{N}_c(\mathbf{t}|\hat{\mathbf{t}}^+, \mathbf{v}_t^+) = \text{Proj}_{\mathbf{t}} \left[\int_{\mathbf{x}} p(\mathbf{t}|\mathbf{x}) \mathcal{N}_c(\mathbf{x}|\mathbf{m}_0^+, \mathbf{v}_0^+) \right. \\ & \quad \left. \cdot \mathcal{N}_c(\mathbf{t}|\mathbf{m}_1^-, \mathbf{v}_1^-) d\mathbf{x} \right] \end{aligned} \quad (71)$$

The integral above can be computed as

$$\begin{aligned} & \int_{\mathbf{x}} p(\mathbf{t}|\mathbf{x}) \mathcal{N}_c(\mathbf{x}|\mathbf{m}_0^+, \mathbf{v}_0^+) \mathcal{N}_c(\mathbf{t}|\mathbf{m}_1^-, \mathbf{v}_1^-) d\mathbf{x} \\ = & \int_{\mathbf{x}} \delta(\mathbf{t} - \mathbf{H}\mathbf{x}) \mathcal{N}_c(\mathbf{x}|\mathbf{m}_0^+, \mathbf{v}_0^+) \mathcal{N}_c(\mathbf{H}\mathbf{x}|\mathbf{m}_1^-, \mathbf{v}_1^-) d\mathbf{x} \end{aligned} \quad (72)$$

$$\propto \int_{\mathbf{x}} \delta(\mathbf{t} - \mathbf{H}\mathbf{x}) \mathcal{N}_c(\mathbf{x}|\mathbf{x}^+, \mathbf{Q}_x^+) d\mathbf{x} \quad (73)$$

where

$$\mathbf{Q}_x^+ = (\mathbf{H}^H \text{Diag}(\mathbf{1} \odot \mathbf{v}_1^-) \mathbf{H} + \text{Diag}(\mathbf{1} \odot \mathbf{v}_0^+))^{-1} \quad (74)$$

$$\mathbf{x}^+ = \mathbf{Q}_x^+ (\mathbf{H}^H \text{Diag}(\mathbf{1} \odot \mathbf{v}_1^-) \mathbf{m}_1^- + \mathbf{m}_0^+ \odot \mathbf{v}_0^+) \quad (75)$$

The integration in (73) actually yields a Gaussian density, whose mean and covariance are $\mathbf{H}\mathbf{x}^+$ and $\mathbf{H}\mathbf{Q}_x^+ \mathbf{H}^H$, respectively. Given this, the projection result then becomes

$$\hat{\mathbf{t}}^+ = \mathbf{H}\mathbf{x}^+ \quad (76)$$

$$\mathbf{v}_t^+ = \text{diag}(\mathbf{H}\mathbf{Q}_x^+ \mathbf{H}^H) \quad (77)$$

and we could further compute the extrinsic message

$$\mathcal{N}_c(\mathbf{t}|\mathbf{m}_1^+, \mathbf{v}_1^+) \propto \frac{\mathcal{N}_c(\mathbf{t}|\hat{\mathbf{t}}^+, \mathbf{v}_t^+)}{\mathcal{N}_c(\mathbf{t}|\mathbf{m}_1^-, \mathbf{v}_1^-)} \quad (78)$$

where

$$\mathbf{v}_1^+ = \mathbf{1} \odot (\mathbf{1} \odot \mathbf{v}_t^+ - \mathbf{1} \odot \mathbf{v}_1^-) \quad (79)$$

$$\mathbf{m}_1^+ = \mathbf{v}_1^+ \odot (\hat{\mathbf{t}}^+ \odot \mathbf{v}_t^+ - \mathbf{m}_1^- \odot \mathbf{v}_1^-) \quad (80)$$

We continue with the factor node $p(\mathbf{y}|\mathbf{t})$, i.e., Module B,

$$\mathcal{N}_c(\mathbf{y}|\hat{\mathbf{y}}^+, \mathbf{v}_y^+) = \text{Proj}_{\mathbf{y}} [\mathcal{N}_c(\mathbf{y}|\mathbf{m}_2^-, \mathbf{v}_2^-) \mathcal{P}(\mathbf{y})] \quad (81)$$

where $\mathcal{P}(\mathbf{y}) \triangleq \int_{\mathbf{t}} p(\mathbf{y}|\mathbf{t}) \mathcal{N}_c(\mathbf{t}|\mathbf{m}_1^+, \mathbf{v}_1^+) d\mathbf{t}$, and the result is

$$\hat{\mathbf{y}}^+ = \mathbb{E}[\mathbf{y}|\mathbf{m}_2^-, \mathbf{v}_2^-, \mathcal{P}(\cdot)] \quad (82)$$

$$\mathbf{v}_y^+ = \text{Var}[\mathbf{y}|\mathbf{m}_2^-, \mathbf{v}_2^-, \mathcal{P}(\cdot)] \quad (83)$$

So, the extrinsic message can now be computed as

$$\mathcal{N}_c(\mathbf{y}|\mathbf{m}_2^+, \mathbf{v}_2^+) \propto \frac{\mathcal{N}_c(\mathbf{y}|\hat{\mathbf{y}}^+, \mathbf{v}_y^+)}{\mathcal{N}_c(\mathbf{y}|\mathbf{m}_2^-, \mathbf{v}_2^-)} \quad (84)$$

$$\mathbf{v}_2^+ = \mathbf{1} \odot (\mathbf{1} \odot \mathbf{v}_y^+ - \mathbf{1} \odot \mathbf{v}_2^-) \quad (85)$$

$$\mathbf{m}_2^+ = \mathbf{v}_2^+ \odot (\hat{\mathbf{y}}^+ \odot \mathbf{v}_y^+ - \mathbf{m}_2^- \odot \mathbf{v}_2^-) \quad (86)$$

So far, we have completed a back and a forward passing. Connecting the two, we attain an iteration of the algorithm.

APPENDIX B PARTICULAR CASES

A. Finite-Resolution Case

In this case we are interested in the case where the observation \mathbf{y} is acquired through a complex-valued quantizer $Q_c(\cdot)$. Specifically, each complex-valued quantizer $Q_c(\cdot)$ consists of two real-valued B -bit quantizers $Q(\cdot)$, which is defined as

$$y_a = Q_c(y_a) \triangleq Q(\Re[y_a]) + \mathbb{J}Q(\Im[y_a]). \quad (87)$$

Hence, the resulting quantized signal \mathbf{y} is given by

$$\mathbf{y} = Q_c(\mathbf{t} + \mathbf{w}) \quad (88)$$

where $\mathbf{w} \sim \mathcal{N}_c(\mathbf{0}, \sigma_w^2 \mathbf{I})$ represents the AWGN. Let $\text{up}(\cdot)$ and $\text{low}(\cdot)$ denote, respectively, the upper and lower boundaries of the quantization interval in which the received value y_a falls, then the transition probability $p(y_a|z_a)$ of interest can be expressed as

$$p(y_a|t_a) = \left[\Phi \left(\frac{\text{up}(\Re[y_a]) - \Re[t_a]}{\sigma_w/\sqrt{2}} \right) - \Phi \left(\frac{\text{low}(\Re[y_a]) - \Re[t_a]}{\sigma_w/\sqrt{2}} \right) \right] \cdot \left[\Phi \left(\frac{\text{up}(\Im[y_a]) - \Im[t_a]}{\sigma_w/\sqrt{2}} \right) - \Phi \left(\frac{\text{low}(\Im[y_a]) - \Im[t_a]}{\sigma_w/\sqrt{2}} \right) \right] \quad (89)$$

with $\Phi(\cdot)$ being the standard Gaussian CDF. To see how these boundaries look like, take uniform quantization as an example and consider a step size of Δ , the quantization output is then given as below (for ease of notation, we abuse the notation y_a to denote $\Re[y_a]$ and $\Im[y_a]$)

$$y_a \in \left\{ (-1/2 + b) \triangleq; b = -2^{B-1} + 1, \dots, 2^{B-1} \right\} \quad (90)$$

with the lower and upper boundaries being

$$\begin{aligned} \text{low}(y_a) &= \begin{cases} y_a - \Delta/2 & \text{if } y_a \geq -(2^{B-1} - 1)\Delta, \\ -\infty & \text{otherwise.} \end{cases} \\ \text{up}(y_a) &= \begin{cases} y_a + \Delta/2 & \text{if } y_a \leq (2^{B-1} - 1)\Delta, \\ +\infty & \text{otherwise.} \end{cases} \end{aligned} \quad (91)$$

Under such a uniform quantization setting, the two equation

$$\mathcal{L}(\mathbf{t}) \triangleq \int_{\mathbf{y}} p(\mathbf{y}|\mathbf{t}) \mathcal{N}_c(\mathbf{y}|\mathbf{m}_2^-, \mathbf{v}_2^-) d\mathbf{y},$$

$$\mathcal{P}(\mathbf{y}) \triangleq \int_{\mathbf{t}} p(\mathbf{y}|\mathbf{t}) \mathcal{N}_c(\mathbf{t}|\mathbf{m}_1^+, \mathbf{v}_1^+) d\mathbf{t},$$

B. Infinite-Resolution Case

AWGN case

$$\mathcal{N}_c(\mathbf{t}|\hat{\mathbf{t}}^-, \mathbf{v}_t^-)$$

$$= \text{Proj}_{\mathbf{t}} \left[\mathcal{N}_c(\mathbf{t}|\mathbf{m}_1^+, \mathbf{v}_1^+) \int_{\mathbf{y}} p(\mathbf{y}|\mathbf{t}) \mathcal{N}_c(\mathbf{y}|\mathbf{m}_2^-, \mathbf{v}_2^-) d\mathbf{y} \right] \quad (92)$$

$$\propto \mathcal{N}_c(\mathbf{t}|\mathbf{m}_1^+, \mathbf{v}_1^+) \mathcal{N}_c(\mathbf{t}|\mathbf{m}_2^-, \sigma_1^2 \mathbf{1} + \mathbf{v}_2^-) \quad (93)$$

After using the Gaussian reproduction property, it becomes

$$\mathbf{v}_t^- = \mathbf{1} \odot (\mathbf{1} \odot \mathbf{v}_1^+ + \mathbf{1} \odot (\sigma_1^2 \mathbf{1} + \mathbf{v}_2^-)) \quad (94)$$

$$\hat{\mathbf{t}}^- = \mathbf{v}_t^- \odot (\mathbf{m}_1^+ \odot \mathbf{v}_1^+ + \mathbf{m}_2^- \odot (\sigma_1^2 \mathbf{1} + \mathbf{v}_2^-)) \quad (95)$$

Given $p(\mathbf{y}|\mathbf{t}) = \mathcal{N}_c(\mathbf{y}|\mathbf{t}^-, \sigma_1^2 \mathbf{1})$, the integral above becomes

$$\begin{aligned} & \int_{\mathbf{t}} p(\mathbf{y}|\mathbf{t}) \mathcal{N}_c(\mathbf{t}|\mathbf{m}_1^+, \mathbf{v}_1^+) \mathcal{N}_c(\mathbf{y}|\mathbf{m}_2^-, \mathbf{v}_2^-) d\mathbf{t} \\ & \propto \mathcal{N}_c(\mathbf{y}|\mathbf{m}_2^-, \mathbf{v}_2^-) \mathcal{N}_c(\mathbf{y}|\mathbf{m}_1^+, \mathbf{v}_1^+ + \sigma_1^2 \mathbf{1}) \end{aligned} \quad (96)$$

$$\mathbf{v}_y^+ = \mathbf{1} \odot (\mathbf{1} \odot \mathbf{v}_2^- + \mathbf{1} \odot (\mathbf{v}_1^+ + \sigma_1^2 \mathbf{1})) \quad (97)$$

$$\hat{\mathbf{y}}^+ = \mathbf{v}_y^+ \odot (\mathbf{r}_1^+ \odot (\mathbf{v}_1^+ + \sigma_1^2 \mathbf{1}) + \mathbf{m}_2^- \odot \mathbf{v}_2^-) \quad (98)$$

REFERENCES

- [1] T. L. Marzetta, "Noncooperative cellular wireless with unlimited numbers of base station antennas," *IEEE Transactions on Wireless Communications*, vol. 9, no. 11, pp. 3590–3600, November 2010.
- [2] E. G. Larsson, O. Edfors, F. Tufvesson, and T. L. Marzetta, "Massive mimo for next generation wireless systems," *IEEE Communications Magazine*, vol. 52, no. 2, pp. 186–195, February 2014.
- [3] J. Hoydis, S. ten Brink, and M. Debbah, "Massive mimo in the ul/dl of cellular networks: How many antennas do we need?" *IEEE Journal on Selected Areas in Communications*, vol. 31, no. 2, pp. 160–171, February 2013.
- [4] D. L. Donoho, A. Maleki, and A. Montanari, "Message-passing algorithms for compressed sensing," *Proceedings of the National Academy of Sciences*, vol. 106, no. 45, pp. 18914–18919, 2009.
- [5] T. P. Minka, "A family of algorithms for approximate bayesian inference," Ph.D. dissertation, MIT, 2001.
- [6] M. Opper and O. Winther, "Expectation consistent approximate inference," *Journal of Machine Learning Research*, vol. 6, no. Dec, pp. 2177–2204, 2005.
- [7] S. Rangan, "Generalized approximate message passing for estimation with random linear mixing," *CoRR*, vol. abs/1010.5141, 2010. [Online]. Available: <http://arxiv.org/abs/1010.5141>
- [8] J. T. Parker, P. Schniter, and V. Cevher, "Bilinear generalized approximate message passing - part I: derivation," *IEEE Trans. Signal Processing*, vol. 62, no. 22, pp. 5839–5853, 2014. [Online]. Available: <https://doi.org/10.1109/TSP.2014.2357776>
- [9] —, "Bilinear generalized approximate message passing - part II: applications," *IEEE Trans. Signal Processing*, vol. 62, no. 22, pp. 5854–5867, 2014. [Online]. Available: <https://doi.org/10.1109/TSP.2014.2357773>
- [10] A. K. Fletcher, M. Sahraee-Ardakan, S. Rangan, and P. Schniter, "Expectation consistent approximate inference: Generalizations and convergence," *CoRR*, vol. abs/1602.07795, 2016. [Online]. Available: <http://arxiv.org/abs/1602.07795>
- [11] H. He, C. K. Wen, and S. Jin, "Generalized expectation consistent signal recovery for nonlinear measurements," in *2017 IEEE International Symposium on Information Theory (ISIT)*, June 2017, pp. 2333–2337.
- [12] —, "Bayesian optimal data detector for hybrid mmwave mimo-ofdm systems with low-resolution adcs," *IEEE Journal of Selected Topics in Signal Processing*, pp. 1–1, 2018.
- [13] M. Bayati and A. Montanari, "The dynamics of message passing on dense graphs, with applications to compressed sensing," *IEEE Transactions on Information Theory*, vol. 57, no. 2, pp. 764–785, Feb 2011.
- [14] S. Wu, L. Kuang, Z. Ni, J. Lu, D. Huang, and Q. Guo, "Low-complexity iterative detection for large-scale multiuser mimo-ofdm systems using approximate message passing," *IEEE Journal of Selected Topics in Signal Processing*, vol. 8, no. 5, pp. 902–915, Oct 2014.
- [15] C. K. Wen, S. Jin, K. K. Wong, J. C. Chen, and P. Ting, "Channel estimation for massive mimo using gaussian-mixture bayesian learning," *IEEE Transactions on Wireless Communications*, vol. 14, no. 3, pp. 1356–1368, March 2015.
- [16] C. K. Wen, C. J. Wang, S. Jin, K. K. Wong, and P. Ting, "Bayes-optimal joint channel-and-data estimation for massive mimo with low-precision adcs," *IEEE Transactions on Signal Processing*, vol. 64, no. 10, pp. 2541–2556, May 2016.
- [17] Y. Qi and T. P. Minka, "Window-based expectation propagation for adaptive signal detection in flat-fading channels," *IEEE Transactions on Wireless Communications*, vol. 6, no. 1, pp. 348–355, Jan 2007.
- [18] J. Cspedes, P. M. Olmos, M. Snchez-Fernndez, and F. Perez-Cruz, "Expectation propagation detection for high-order high-dimensional mimo systems," *IEEE Transactions on Communications*, vol. 62, no. 8, pp. 2840–2849, Aug 2014.
- [19] J. N. Laneman, D. N. C. Tse, and G. W. Wornell, "Cooperative diversity in wireless networks: Efficient protocols and outage behavior," *IEEE Transactions on Information Theory*, vol. 50, no. 12, pp. 3062–3080, Dec 2004.
- [20] S. Jin, X. Liang, K. K. Wong, X. Gao, and Q. Zhu, "Ergodic rate analysis for multipair massive mimo two-way relay networks," *IEEE Transactions on Wireless Communications*, vol. 14, no. 3, pp. 1480–1491, March 2015.
- [21] R. Zhao, Y. Huang, W. Wang, and V. K. N. Lau, "Ergodic achievable secrecy rate of multiple-antenna relay systems with cooperative jamming," *IEEE Transactions on Wireless Communications*, vol. 15, no. 4, pp. 2537–2551, April 2016.

- [22] A. K. Fletcher and S. Rangan, "Inference in deep networks in high dimensions," *CoRR*, vol. abs/1706.06549, 2017. [Online]. Available: <http://arxiv.org/abs/1706.06549>
- [23] H. Zhang and et al, "Multi-layer generalized expectation consistent approximate bayesian inference," 2018, in preparation.
- [24] S. Rangan, P. Schniter, and A. K. Fletcher, "Vector approximate message passing," *CoRR*, vol. abs/1610.03082, 2016. [Online]. Available: <http://arxiv.org/abs/1610.03082>
- [25] P. Lioliou, M. Viberg, and M. Matthaiou, "Bayesian approach to channel estimation for af mimo relaying systems," *IEEE Journal on Selected Areas in Communications*, vol. 30, no. 8, pp. 1440–1451, September 2012.
- [26] X. Meng, S. Wu, L. Kuang, and J. Lu, "An expectation propagation perspective on approximate message passing," *IEEE Signal Processing Letters*, vol. 22, no. 8, pp. 1194–1197, Aug 2015.
- [27] B. Çakmak and M. Opper, "Expectation propagation for approximate inference: Free probability framework," *CoRR*, vol. abs/1801.05411, 2018. [Online]. Available: <http://arxiv.org/abs/1801.05411>
- [28] C. E. Rasmussen, "Gaussian processes in machine learning," in *Advanced lectures on machine learning*. Springer, 2004, pp. 63–71.